INTERNAL AND SURFACE PHENOMENA IN METAL COMBUSTION

Edward L. Dreizin
AeroChem Research Laboratories, Inc., Princeton, New Jersey

Irina E. Molodetsky and Chung K. Law
Princeton University, Princeton, New Jersey

Introduction

Combustion of metals has been widely studied in the past, primarily because of their high oxidation enthalpies. A general understanding of metal combustion has been developed based on the recognition of the existence of both vapor-phase and surface reactions and involvement of the reaction products in the ensuing heterogeneous combustion. However, distinct features often observed in metal particle combustion, such as brightness oscillations and jumps (spearpoints), disruptive burning, and non-symmetric flames are not currently understood.

Recent metal combustion experiments using uniform high-temperature metal droplets produced by a novel micro-arc technique (ref. 1-3) have indicated that oxygen dissolves in the interior of burning particles of certain metals and that the subsequent transformations of the metal-oxygen solutions into stoichiometric oxides are accompanied with sufficient heat release to cause observed brightness and temperature jumps. Similar oxygen dissolution has been observed in recent experiments on bulk iron combustion (ref. 4, 5) but has not been associated with such dramatic effects.

This research addresses heterogeneous metal droplet combustion, specifically focusing on oxygen penetration into the burning metal droplets, and its influence on the metal combustion rate, temperature history, and disruptive burning.

A unique feature of the experimental approach is the combination of the microgravity environment with a novel micro-arc GEnerator of Monodispersed MEtal Droplets (GEMMED), ensuring repeatable formation and ignition of uniform metal droplets with controllable initial temperature and velocity. The droplet initial temperatures can be adjusted within a wide range from just above the metal melting point, which provides means to ignite droplets instantly upon entering an oxygen containing environment. Initial droplet velocity will be set equal to zero allowing one to organize metal combustion microgravity experiments in a fashion similar to usual microgravity liquid fuel droplet combustion studies. In addition, the internal compositions of rapidly quenched metal particles will be analyzed using SEM technique. Such compositions are similar to those existing during the combustion and provide new insight on metal combustion processes. The results of this experimental work will be used to model the fundamental mechanisms of metal combustion.

Preliminary experimental results on Al and Zr particle combustion at normal gravity are discussed here. This work was initiated in July, 1994.

Experimental

Metal particle combustion experiments were conducted using the GEMMED described elsewhere (ref. 6). The GEMMED uses a pulsed micro-arc discharge to melt the edge of a consumable wire electrode and separate molten droplets from the wire. Each metal droplet is formed and ignited in a single micro-arc pulse. Repeatability of the duration, current, and voltage of the micro-arc pulses results in reproducible diameters, temperatures, and velocities of the metal droplets formed.

The color temperature histories of the burning droplets were recorded using a three-wavelength pyrometer. The pyrometer included an iris, a fiber optics trifurcated bundle, three interference filters, and three HC120-01 Hamamatsu photo-sensor modules. Different wavelengths of the interference filters were chosen for each metal so that no bands which are observed in the metal-oxygen (or metal-nitrogen) spectra could contribute to the measured signals. The pyrometer was calibrated using a tungsten strip lamp, providing a maximum black body temperature of 2650 K. For any time during the particle trajectory, two color temperatures could be deduced from the three recorded radiation signals. This provided a criterion for the correctness of the temperature measurements, e.g., agreement of the two inferred temperatures showing that the radiation spectrum is that of a gray body, validated the color temperatures.

Spatial resolution of the optical signals produced by the particle and the external luminous zone was achieved using a slot array with equally spaced 0.2 mm wide slots positioned between the burning particle trajectory and the pyrometer (close to the particle trajectory) with the slots perpendicular to the particle velocity vector. The radiation from burning particles moving behind the array was registered as a series of pulses. Each radiation pulse was formed when a particle surrounded with a luminous zone, crossed a single slot. Detailed comparisons of the two temperature-versus-time curves inferred from the three radiation pulses simultaneously measured at different wavelengths were conducted in order to separate particle and stand-off luminous zone radiations and identify the particle temperature. Such analyses showed that a period existed when the two temperatures agreed well for each radiation pulse corresponding to a burning particle crossing a single slot. This period, as expected, was close to the time needed for the particle (excluding the external luminous zone) to cross the slot. Thus, the particle surface temperature could be measured when burning particles crossed the slot, and most of the flame radiation was blocked.

The luminous zone shape was visualized by video-recording of the combustion events using a free running camera at a fast shutter speed (0.5 ms exposure time). Particles were quenched on glass slides at different combustion times, and the shapes of smoke traces surrounding the quenched particles were examined and compared with the video-camera images.

Rapid particle quenching was used to freeze the particle internal compositions which existed during the combustion. The fast cooling rate of a metal droplet provided by its impinging onto a cool metal surface, was utilized in this work. To minimize the particle shape distortion, a thin Al foil was used as a quenching substrate, which resulted in the particle welding into the foil upon collision. The quenched particles were embedded into epoxy and cross-sectioned. An electron probe microanalyzer "Cameca SX50" was used for the cross-section examination, and Energy-Dispersive Spectroscopy (EDS) (Princeton Gamma Tech. detector) as well as Wavelength-Dispersive Spectroscopy (WDS) scan were utilized to determine the particle internal compositions.

Results

Combustion of 80, 120, 165, and 200 μm diameter Al particles and 240 μm diameter Zr particles in room air have been studied.

Video recordings of metal particle combustion events as well as spatially resolved radiation measurements using the slot array consistently showed the existence of luminous zones surrounding burning particles of both Al and Zr. The estimated sizes of the luminous zones correlated well with the sizes of smoke clouds deposited when the particles were quenched on glass slides. For both Al and Zr, the clouds formed upon ignition were spherically symmetric but lost their symmetry later in the combustion. The comparison of the luminous zone (or cloud) shapes with the radiation intensity signals measured in separate channels of the three-wavelength pyrometer indicated that for both metals the zones became non-symmetric after the maxima of radiation were reached.

Pronounced oscillations of radiation intensity caused by the spinning of burning Al particles began simultaneously with the deformation of the originally symmetric external luminous zone. Al droplet combustion also was accompanied by separation of small satellites and often ended with explosions, although smooth particle extinguishing was observed in some cases. Burning Zr particles did not exhibit such noticeable oscillations but their combustion in air always terminated by strong explosions.

Temperature histories of 165 μm diameter Al and 240 μm diameter Zr particles burning in air are shown in Fig. 1. Solid curves in Fig. 1 represent temperature histories determined for single particle combustion events without using the slot array. These temperature histories were very reproducible. For reference, important phase transition temperatures are indicated as dashed lines in Fig. 1. While the two temperatures inferred from the three measured radiation signals were consistent for Al particles (an example of only one of the temperature histories is shown in Fig. 1a), there was some inconsistency between the two temperatures determined for burning Zr particles without the slot array. An example of the temperature history $T_1(t)=f\{$(radiation intensity at 589nm)/(radiation intensity at 510nm)$\}$ of a single Zr particle burning in air is shown in Fig. 1 (solid line) along with the temperatures measured using several (reproducible) Zr particles crossing the slot array (triangles). Each triangle shows where the two temperatures became consistent for different pulses recorded for single particles crossing the slots.

The maximum temperature of burning Al particles, Fig. 1a, was measured during the initial combustion period and exceeded the Al boiling point (2520°C), indicating that particle radiation was shielded by the radiation of spherically symmetric stand-off flame zone. Later on, the temperature stabilized slightly below the Al boiling point (but above the boiling temperature of the saturated Al-O solution, ref. 7), and then decreased close to the solidification point of Al_2O_3 (2050°C) immediately before the extinguishment. Maximum temperatures of Zr particles burning in air were always below the ZrO_2 melting point (2700°C), Fig. 1b and approached the temperature of eutectic αZr and ZrO_2 formation ($\sim$2000°C) at the completion of combustion.

EDS and WDS determination of the internal compositions of rapidly quenched Al and Zr particles revealed the presence of oxygen in particle interiors for both metals, while no oxide shells or inclusions were observed. Internal compositions of particles quenched at different times are shown in Fig. 2. Measured atomic concentrations of oxygen in Al particles did not exceed 14%, Fig. 2a, until "oxide caps" started to grow after approximately of 2/3 of the entire particle combustion time. The "oxide cap" compositions were close to the stoichiometric Al_2O_3 with some traces of nitrogen, while the composition of the rest of Al particle did not change. The composition of burning Zr particles follows a different path, incorporating both nitrogen and oxygen. Gradual growth of oxygen concentration, approaching stoichiometric ZrO_2 at the combustion end, was observed (see Fig. 2b). Nitrogen concentration in Zr particles was observed to increase up to 20% and then to fall during combustion.

Discussion

According to the existing metal combustion classification, the two metals experimentally examined in this work belong to different groups: Al is a vapor-phase burner, while Zr is known to burn heterogeneously. However, some striking similarities were observed in their burning behavior:

1) symmetric stand-off luminous zones formed in both cases and eventually became non-symmetric;
2) oxygen dissolved in the burning metal droplets with no observed oxide shell formation;
3) disruptive burning occurred with both metals.

The presence of oxygen in the particle interiors and the absence of oxide shells suggest that not only the surface of the burning metal droplets, but also, their entire interiors are actively involved in the combustion processes. It means that metal-gas interactions in the condensed phase should be analyzed in addition to vapor-phase and surface metal-gas interactions in order to elucidate metal particle combustion behavior. Interactions of materials in the condensed phase are usually described using concentration versus temperature phase diagrams. The Al-O and Zr-O phase diagrams suggest that although stoichiometric oxide phases (e.g., liquid Al_2O_3 or solid ZrO_2) are stable as individual phases at the combustion temperatures, no oxides can be formed in a binary metal-oxygen system until a certain limit of oxygen concentration is reached. Thus, while the conventional heterogeneous metal combustion model assumes that an oxide forms as a result of a surface reaction occurring when a clean high-temperature metal surface is exposed to an oxygen-containing environment, the phase diagrams suggest that a metal-oxygen solution forms until the oxygen concentration attains the solubility limit. Then, assuming further oxygen availability, a transition from the saturated solution to the stoichiometric oxide (liquid or solid) can occur. Such a transition is exothermic, but at thermodynamic equilibrium takes place at a constant temperature. However, even at the equilibrium, it can be associated with changes of internal structure and void/crack formation, gas release, etc., which may cause brightness and temperature jumps and particle explosions.

Specifically, the Al-O phase diagram (ref. 7) suggests that liquid Al-O solutions and a vapor-phase form at temperatures from 2240 to 2460°C and at atomic oxygen concentrations below ~14%. Liquid Al_2O_3 starts to form when the 14% limit is attained, and both liquid Al and liquid Al_2O_3 coexist in the temperature range of 2050-2240°C. Thus, the transition from solution to Al_2O_3 can occur when the internal oxygen content is close to 14% and the temperature is in the range of 2240-2460°C. These conditions are in good agreement with the particle temperatures and internal oxygen concentrations measured in Al combustion tests at the transition from the spherically symmetric to non-symmetric combustion mode, associated with disruptive events and particle spinning.

The binary Zr-O system forms liquid solutions at temperatures above 2000°C with the oxygen solubility limit increasing from 40 to 66% (atomic) as the temperature increases up to 2700°C (ref. 7). Solid ZrO_2 forms when the solubility limit is reached, and it co-exists with the saturated solution. Therefore, the transition from solution to oxide can occur if the internal oxygen content exceeds 40% and the temperature is above 2000°C. These conditions, again, correlate well with the Zr particle temperature and composition measured prior to the observed explosions.

Thus, while the possible mechanisms (such as gas release, oxygen penetration into forming voids, or non-equilibrium oxide formation) for the observed phenomena of disruptive burning, explosion, or spearpoint, should be elaborated for each case separately, the generic mechanism actuating these processes apparently is the solution-oxide transformations discussed here. Such transformations actually represent oxidation reactions developing inside burning metal particles and should be added to conventionally considered external (vapor-phase) and surface oxidation processes.

Summary and Plans

Preliminary normal gravity experiments on metal combustion have shown that oxygen dissolves in burning Al and Zr particles. It is suggested that the transformation of a metal-oxygen solution into the stoichiometric oxide results in observed particle brightness and temperature jumps and explosions.

Further work will focus on the experimental apparatus modification for microgravity tests and the design of microgravity experiments. Following experimental tests will elucidate the role of external transport processes on metal particle combustion and, in particular, those processes resulting in non-symmetric luminous zone formation.

Acknowledgements

The research performed at AeroChem and Princeton University were respectively supported by the Microgravity Science and Application Division of NASA (Lewis RC) and by the Office of Naval Research. The authors appreciate the help of Dr. E. Vicenzy of Princeton Material Institute in the SEM sample analyses.

References

1. Dreizin, E.L., Suslov, A.V. and Trunov, M.A., *Combust. Sci. Tech.* 87:45-58 (1992).
2. Dreizin, E.L., Suslov, A.V. and Trunov, M.A., *Combust. Sci. Tech.* 90:79-99 (1993).
3. Dreizin, E.L. and Trunov, M.A., *Combustion and Flame*, in press (1995).
4. Steinberg, T.A., Wilson, D.B., and Benz, F., *Combustion and Flame*, 88:309-320 (1992).
5. Steinberg, T.A., Mulholland, G.P., Wilson, D.B., and Benz, F., *Combustion and Flame*, 89:221-228 (1992).
6. Suslov, A.V., Dreizin, E.L. and Trunov, M.A., *Powder Tech.*, 74:23-30 (1993).
7. Levinskiy, Y.V., *P-T-X Binary Phase Diagrams of Metal Systems*, Moscow, Metallurgia, (1990) (In Russian).

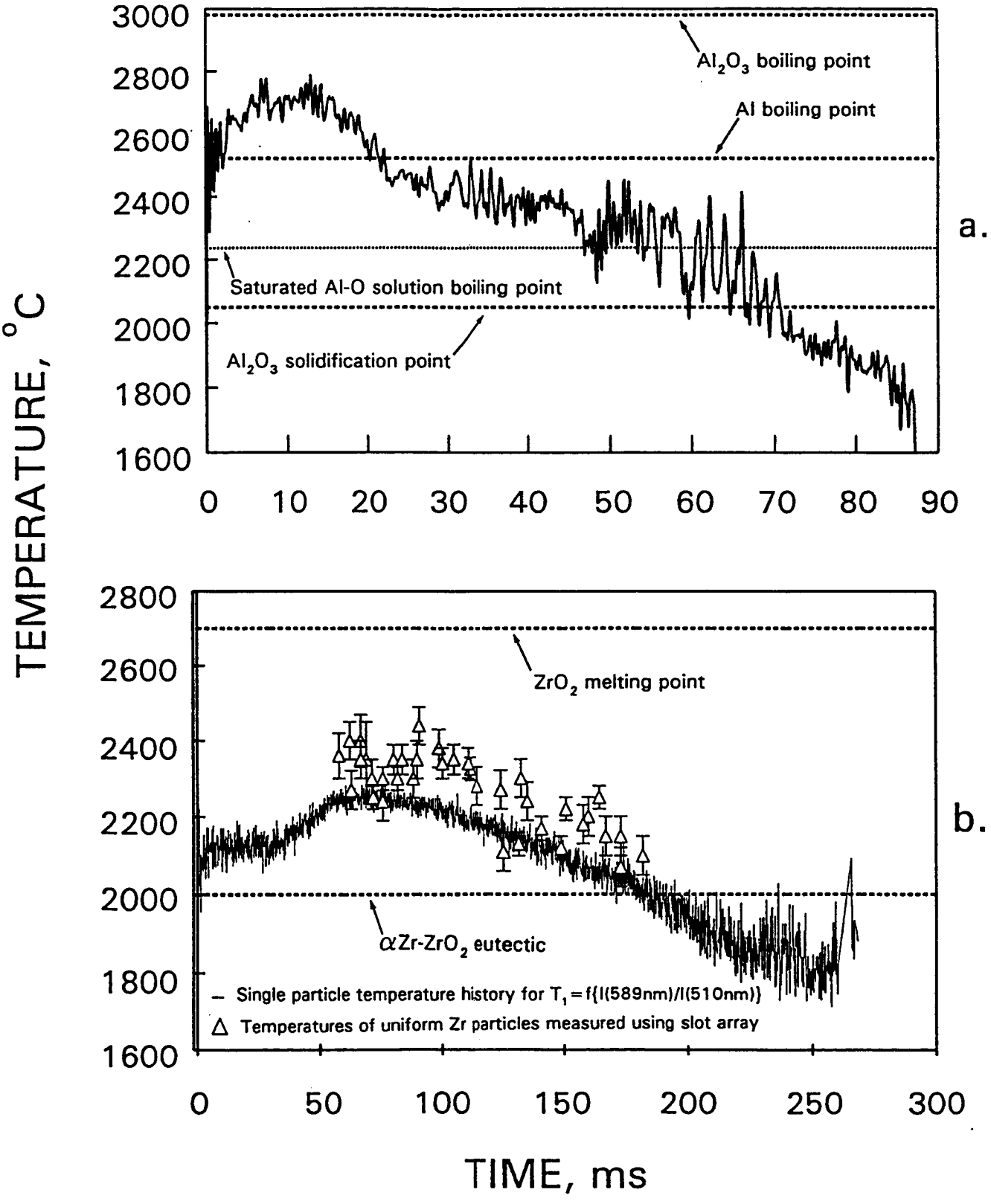

FIGURE 1 TEMPERATURE HISTORIES OF BURNING METAL PARTICLES

(a) Al, Initial Diameter 165 μm
(b) Zr, Initial Diameter 240 μm

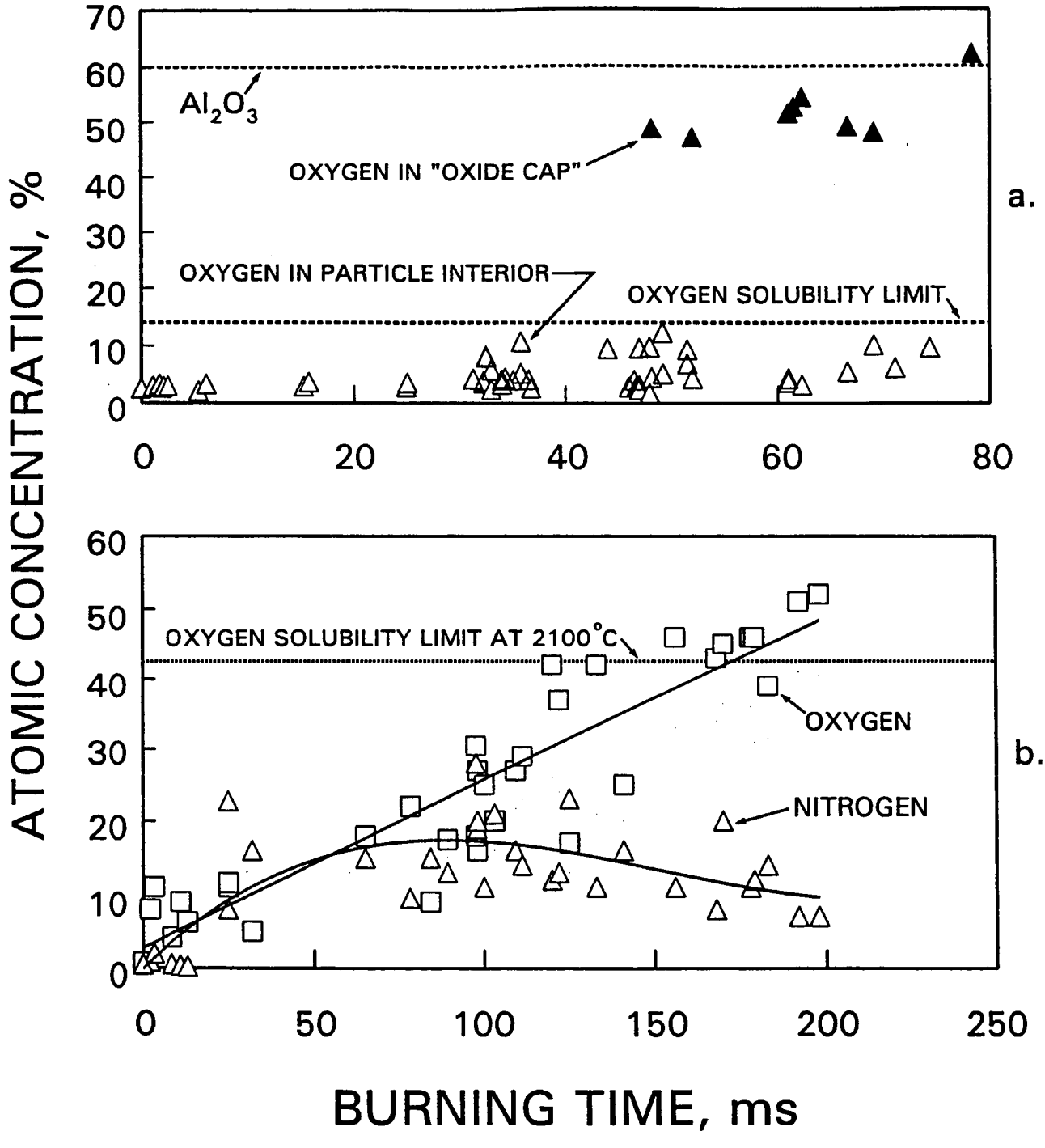

FIGURE 2 INTERNAL COMPOSITION HISTORIES OF BURNING METAL PARTICLES

(a) Al, Initial Diameter 165 μm
(b) Zr, Initial Diameter 240 μm